



PERGAMON

www.elsevier.com/locate/watres

*Wat. Res.* Vol. 35, No. 3, pp. 750–760, 2001  
© 2001 Elsevier Science Ltd. All rights reserved  
Printed in Great Britain  
0043-1354/01/\$ - see front matter

PII: S0043-1354(00)00295-5

## CATALYTIC DECOMPOSITION OF THE REACTIVE DYE UNIBLUE A ON HEMATITE. MODELING OF THE REACTIVE SURFACE

F. HERRERA<sup>1</sup>, A. LOPEZ<sup>2</sup>, G. MASCOLO<sup>2</sup>, P. ALBERS and J. KIWI<sup>1\*3M</sup>

<sup>1</sup>Institute of Physical Chemistry II, EPFL, 1015 Lausanne, Switzerland; <sup>2</sup>CNR-IRSA Department of Water Chemistry and Technology, Via F de Blasio 5, Bari 70123, Italy and <sup>3</sup>Degussa AG, Wolfgang, D-63403 Hanau 1, Germany

(First received 30 September 1999; accepted in revised form 25 May 2000)

**Abstract**—Experimental results from the adsorption and subsequent catalytic combustion of the reactive dye Uniblue A on hematite indicate that this iron oxide can be used as an affordable catalyst for environmental purposes. Uniblue A was adsorbed on hematite and the products of the catalytic oxidation in O<sub>2</sub> atmosphere were analyzed by thermal programmed gas-chromatography/mass spectrometry (STDS-GC-MS) analysis. The catalytic combustion of Uniblue A in the presence of hematite led to about 40% conversion of the dye C-content into CO<sub>2</sub> at  $T = 275^{\circ}\text{C}$ . The activation energy ( $E_a$ ) for the desorption of CO<sub>2</sub> and other polyaromatic hydrocarbons (PAHs) from the hematite surface was determined to be  $23.4\text{ kcal mol}^{-1}$ . Identification of the species of Uniblue A in solution and those existing on the hematite surface was carried out in the framework of the generalized two-layer diffuse model. The modeling of the amount of dye absorbed on hematite is in good agreement with the experimental data. © 2001 Elsevier Science Ltd. All rights reserved

**Key words**—Uniblue A, catalytic combustion, adsorption, hematite, by-products, modeling

### INTRODUCTION

The treatment of textile dyeing waters by conventional methods such as flocculation, reverse osmosis, activated carbon adsorption, ozonization and advanced oxidation technologies (AOTs) is a common practice but has drawbacks due to the increasing number of refractory materials found in wastewater effluents and the difficulties in the complete removal of color (Pulgarin and Kiwi, 1996; Roques, 1996). The cost of ozonization which is widely used still needs to be reduced for competitiveness.

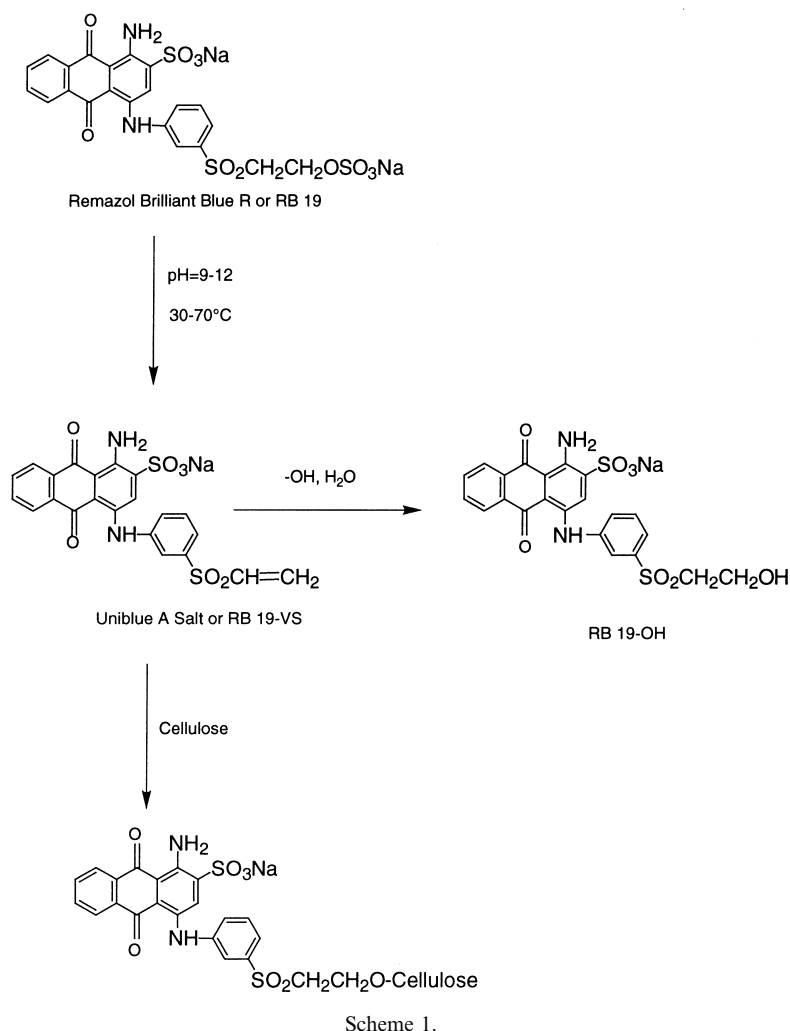
This study addresses an alternative technology for the removal of non-biodegradable reactive dyes like Uniblue A and Remazol Brilliant Blue R (RB19) from textile-mill effluents (Hoechst Portuguesa, 1997). The objective of this research is to explore catalytic combustion after dye absorption on a suitable substrate as a treatment for the destruction of the reactive dye Uniblue A. This study reports on (a) the adsorption process and modeling of the reactive dye species at the catalyst surface, (b) the identification of the gas products generated during the catalytic oxidation and finally (c) the physical characterization of hematite by way of gas adsorp-

tion. Other oxides like goethite, alumina, silica and titania were also screened for the low-temperature catalytic combustion of Uniblue A. Hematite ( $\alpha\text{-Fe}_2\text{O}_3$ ) was found to be the most suitable material combining significant dye adsorption from solution, acceptable kinetic efficiency and stability.

Textile dyes in general are non-biodegradable under aerobic conditions (Zollinger, 1987). During the biological treatment of textile waste waters varying amounts of dyes and their metabolites are sorbed in bioflocs (Ganesh *et al.*, 1994). Reactive dyes are produced in increasing quantities in a variety of colors. They link through chemical bonding to fibers. These dyes are resistant to light degradation, the action of atmospheric gases and oxidants, and some acids and bases. But the same properties that make these dyes suitable dyestuffs, make them difficult to degrade (decolorize) in water bodies. Few studies have been devoted in recent years to the removal of this rather recent generation of reactive dyes like Uniblue A and Remazol Brilliant Blue R (Pasti and Crawford, 1991; Lonergan *et al.*, 1995; Ince *et al.*, 1997; Herrera *et al.*, 1999).

Scheme 1 shows the structure and hydrolysis of Remazol Brilliant Blue (RB19) and the way it is subsequently linked to fibers like cellulose. Scheme 1 shows how RB19 reacts and partly hydrolyses forming a covalent bond with textile fiber/cellulose

\*Author to whom all correspondence should be addressed.  
Tel.: +41-21-693-3621; fax: +41-21-693-3621; e-mail: john.kiwi@epfl.ch



through the vinyl-sulfonate anchor reactive group. This process involves the addition of a nucleophilic -OH group of the fiber to the vinyl-sulfonate through a Michael-type 1,4-nucleophilic addition mechanism. The fixation rate between the reactive dye and the fiber is usually below 90% (Camp and Sturrock, 1990).

## MATERIALS AND METHODS

### Materials

Uniblu A salt was Aldrich 29,640-9 p.a. grade, MW=506.5,  $\lambda_{\max} = 594 \text{ nm}$  with  $\epsilon_{594} = 5570 \text{ M}^{-1} \text{ cm}^{-1}$ . Acid and bases used to adjust the pH were Fluka p.a. and used as received. High surface area  $\alpha\text{-Fe}_2\text{O}_3$  ( $157.6 \text{ m}^2 \text{ g}^{-1}$ ) was prepared according to known procedures (Cornell and Schwertmann, 1980). Transmission electron microscopy (TEM) showed crystals with a narrow size distribution of 20–30 nm.

### Adsorption isotherm

To a solution containing  $\alpha\text{-Fe}_2\text{O}_3$ ,  $400 \text{ mg l}^{-1}$  aliquots of Uniblu A (1.69 mM) were added keeping the pH at 5.5. After the addition of each aliquot of Uniblu A and equilibration during 5–10 min, the solution presented the

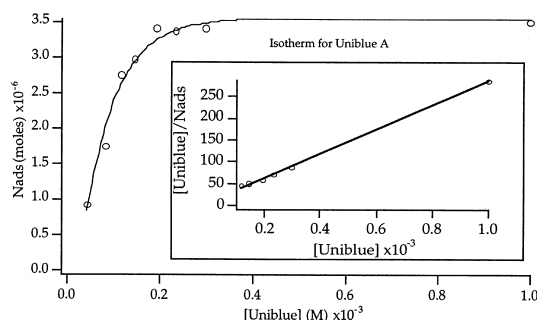


Fig. 1. Adsorption isotherm of Uniblu A on hematite. The inset shows the linearization of the initial part of the Langmuir isotherm. For other details see text.

same molar absorption characteristics for the next 24 h. Independent tests proved that equilibrium was reached within this time period. The suspension containing the hematite and the dye was centrifuged at 14,000 RPM for 15 min. The supernatant containing the non-adsorbed Uniblu A was analyzed spectrophotometrically to determine the concentration of Uniblu A in solution at  $\lambda = 594 \text{ nm}$ . The results are reported in Fig. 1.

### Determination of the $pK_a$ values of Uniblue A and $\alpha\text{-Fe}_2\text{O}_3$

The  $pK_a$  values for Uniblue A and  $\alpha\text{-Fe}_2\text{O}_3$  have been determined with a Titrino DMS 716 titrator of Metrohm AG Herisau, Switzerland. The titration was carried out with a solution of NaOH 0.01 N. The  $pK_a$  values of Uniblue A were: for the sulfonic group  $\sim 1$ , for the primary amine group = 3.97 and for the secondary amino group = 6.37. The two  $pK_a$  values of  $\alpha\text{-Fe}_2\text{O}_3$  were found to be 6.7 and 10.4.

### Catalytic combustion of Uniblue A on hematite

The dye Uniblue A (1.69 mM) was fully adsorbed on hematite ( $0.4\text{ g l}^{-1}$ ) at pH 5.5. This is equivalent to a loading of 2137 mg of Uniblue A per gram hematite. The dye during the adsorption process separates from the solution. After drying, the samples were weighed and put in a cylindrical oven. The samples were introduced into the oven in the form of a tablet. The temperature in the oven and the  $\text{O}_2$  gas flow ( $15\text{ ml min}^{-1}$ ) were stabilized prior to each experiment. Subsequently, the samples were reacted for 30 s at each of the temperatures shown in Fig. 5 and the  $\text{CO}_2$  collected in the vessel provided for this purpose with NaOH. Subsequently, the carbonate was titrated with HCl.

### Concentration of hematite active surface sites

The surface site density was determined from fluoride adsorption. To carry out the measurements a hematite solution containing  $2\text{ g l}^{-1}$  was used and the range of fluoride concentrations was varied from  $1 \times 10^{-5}$  to  $1 \times 10^{-3}\text{ M}$ . The  $\text{F}^-$  concentration in the supernatant solution was determined with the help of a Dionex Ion-Liquid Chromatograph (ICL) provided with an AG14 column. The maximum extent of  $\text{F}^-$  was found by fitting the experimental data to the linearized Langmuir equation.

### BET area and hematite surface parameters

Surface area, pore size diameter, and porosity were determined with a BET Carlo Erba Sorptomatic-1900 unit. The  $\text{N}_2$  desorption isotherm was calculated using the cylindrical pore model of BJH-model (Barret *et al.*, 1951). Hematite presented a surface area of  $157.7\text{ m}^2\text{ g}^{-1}$ .

### Modeling

The ionization of Uniblue A as a function of pH was calculated using the  $pK_a$  values found experimentally via the ChemEQL program (version 2.0. for Macintosh written by B. Muller, Kastanienbaum, Switzerland). The equilibria

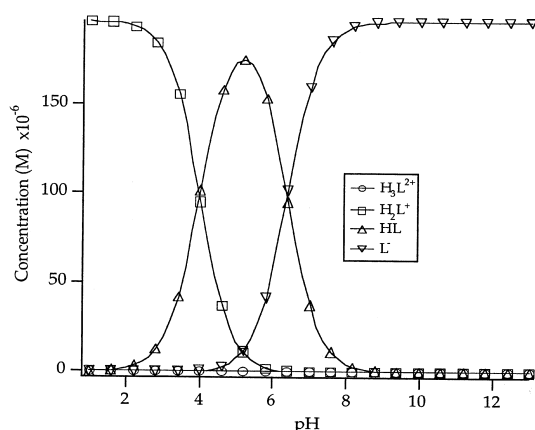
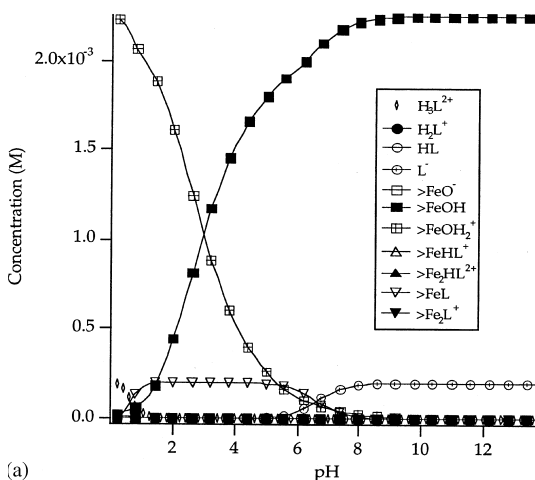


Fig. 2. Distribution of the Uniblue A in solution vs. pH.

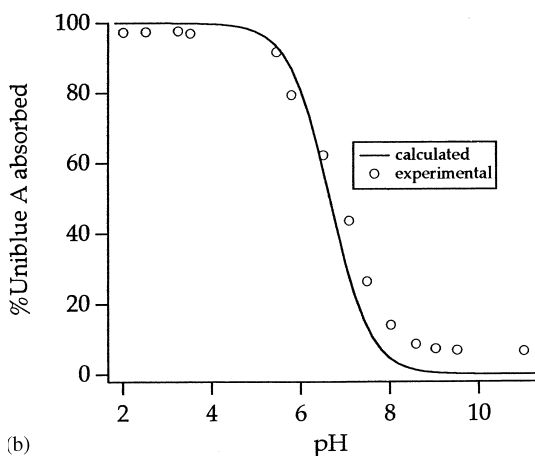
species in the solution were computed by this method. The generalized two-layer diffuse model (diffuse/GTL) has been chosen to account for the electrostatic interaction between dye species at the iron-oxide surface. It takes into account the specific surface area, the iron-oxide surface  $pK_a$  values, the concentration of oxide surface sites and the ionic strength of the solution. The numerical calculations for some of the parameters used in the Chem EQL matrix were carried out with a MatLab 5.2 (Math Works Inc.). The results from these calculations are shown in Figs 2 and 3.

### Adsorption as a function of pH

A known amount of hematite ( $1.5\text{ g l}^{-1}$ ) was added to Uniblue A (0.197 mM) and the pH was adjusted by addition of HCl under continuous stirring. The temperature was maintained at  $22^\circ\text{C}$  in a thermostated bath to avoid losses due to evaporation. After a 15 min equilibration period, aliquots were removed from the suspension and centrifuged at 14,000 RPM for 15 min. The concentration of Uniblue A in the supernatant was determined spectrophotometrically and subtracted from the initial concentration to determine the adsorbed amount.



(a)



(b)

Fig. 3. (a) Uniblue A species existing in solution and hematite surface species as a function of pH. (b) Adsorption of Uniblue A (1.69 mM) on hematite (0.4 g/L) as a function of solution pH. Experimental and calculated values. For other details see text.

*System for thermal degradation studies coupled gas-chromatography and mass-spectrometry (STDS-GC-MS) measurements*

The system has been recently described (Mascolo *et al.*, 1997) and allows the identification of combusted organic species in air. The instrumentation consists of four integrated components: (a) controlling and data acquisition unit, (b) thermal reaction compartment where the air was let in at a flow rate of  $3.0 \text{ ml min}^{-1}$ , (c) cryogenic trapping gas-chromatograph (GC) and finally (d) a quadrupole mass spectrometer. The GC-column used was a Chromopack CP-

SIL 8CB with i.d. = 0.32 mm (60 m length) and 0.25 mm film thickness. The initial temperature of the column was  $60^\circ\text{C}$  and then increased at  $15^\circ\text{C min}^{-1}$  up to  $320^\circ\text{C}$  during the measurements.

In a typical experiment, 2 mg of Uniblue A (by itself or adsorbed on hematite) was placed into a quartz capillary tube (1.5 mm i.d., 15 mm length from Vitro Dynamics, Rochaway, NJ, USA). The quartz tube was inserted into the probe for 5 min periods at the temperatures specified in Tables 1 and 2. The organic compounds formed during the incineration step were transferred and subsequently kept at

Table 1. By products identification during Uniblue combustion by STDS

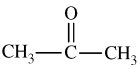
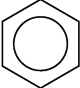
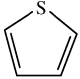
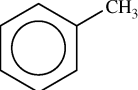
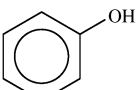
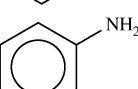
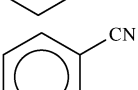
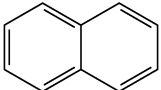
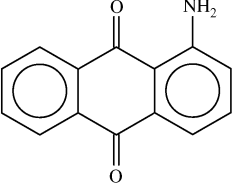
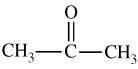
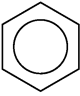
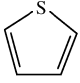
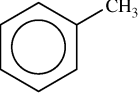
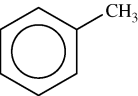
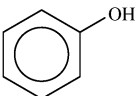
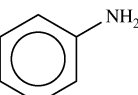
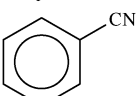
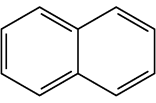
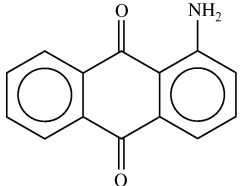
No.	Compound	Retention time	200°C	300°C	375°C	450°C	600°C
1	SO <sub>2</sub>	1-2		X	X	X	
2	CH <sub>3</sub> CHO	6.3			X	X	X
3		10			X	X	
4	CH <sub>3</sub> CN	10.4					X
5		10.6	X	X	X	X	X
6		10.8			X	X	X
7	HCl	11			X	X	
8	CH <sub>3</sub> COOH	11.3				X	
9		12.5			X	X	X
10		15.8	X	X	X	X	X
11		16.4					X
12		17.7			X	X	X
13		18.7			X	X	X
14		29.3					X

Table 2. By-products identification during Uniblu on hematite combustion by STDS

No.	Compound	Retention time	200°C	300°C	375°C	450°C	600°C
1	SO <sub>2</sub>	1–2		X	X	X	X
2	CH <sub>3</sub> CHO	6.3		X	X	X	X
3		10		X	X	X	
4	CH <sub>3</sub> CN	10.4		X	X	X	X
5		10.6	X	X	X	X	X
6		10.8					X
7	HCl	11			X		X
8	CH <sub>3</sub> COOH	11.3			X		
9		12.5		X	X	X	X
10		14.1			X	X	
11		15.8				X	X
12		16.4					X
13		17.7			X	X	X
14		18.7			X	X	X
15		29.3	X	X	X	X	X

250°C to analyze the organic compound without degradation. These compounds were then transferred into the cryogenic trapping GC-chamber where they were focused on a capillary GC column, separated by a temperature gradient and identified by mass spectrometry (MS).

## RESULTS AND DISCUSSION

### Adsorption isotherm experiments

Figure 1 shows the adsorption isotherm of Uniblu A on hematite in a plot of the number of adsorbed

moles ( $N_{\text{ads}}$ ) as a function of the equilibrium concentration of dye used. Details of the determination have been reported (see Materials and methods section). The adsorption has been carried out at pH 5.5. This pH has been chosen after preliminary experiments which revealed that: (a) at pH < 5 dissolution of the iron surface takes place leading to iron-complexes. The absorption of these complexes interferes with the optical absorption of Uniblue A. It was also observed that at pH > 5.5 the adsorption of Uniblue A on hematite begins to decrease with increasing pH (Fig. 3(a)). Figure 1 shows monolayer adsorption of Uniblue A on hematite. The inset of Fig. 1 shows the linearization of the Langmuir isotherm at concentrations of Uniblue A below 0.2 mM. The equilibrium constant for the dye adsorption at the iron-oxide surface can be estimated from

$$\frac{N_{\text{ads}}}{N_{\text{sites}}} = \frac{k_a[\text{Uniblue}]}{k_d + k_a[\text{Uniblue}]} \quad (1)$$

where  $N_{\text{ads}}$  is the number of adsorbed molecules of Uniblue A on  $\alpha\text{-Fe}_2\text{O}_3$ ,  $N_{\text{sites}}$  is the number of  $\alpha\text{-Fe}_2\text{O}_3$  sites,  $k_a$  is the adsorption constant and  $k_d$  is the desorption constant for Uniblue A molecules on  $\alpha\text{-Fe}_2\text{O}_3$ . Linearizing equation (1)

$$\frac{[\text{Uniblue}]}{N_{\text{ads}}} = \frac{N_{\text{sites}}}{K} + \frac{[\text{Uniblue}]}{N_{\text{sites}}} \quad (2)$$

where the equilibrium constant  $K = k_a/k_d$  has a value of  $K = 1.73 \times 10^6 \text{ L mol}^{-1}$ .

#### Uniblue A and hematite speciation in solution

Scheme 2 shows the Uniblue A structure as a function of solution pH in the absence of hematite. In Fig. 3 the  $\text{H}_3\text{L}^{2+}$  is the Uniblue A species in the acid range protonating the two amino groups. The species  $\text{H}_2\text{L}^+$  originates from  $\text{H}_3\text{L}^{2+}$  by losing one proton from the sulfonic group at a  $\text{p}K_a$  around 1. HL originates from the deprotonation of  $\text{H}_2\text{L}^+$  at

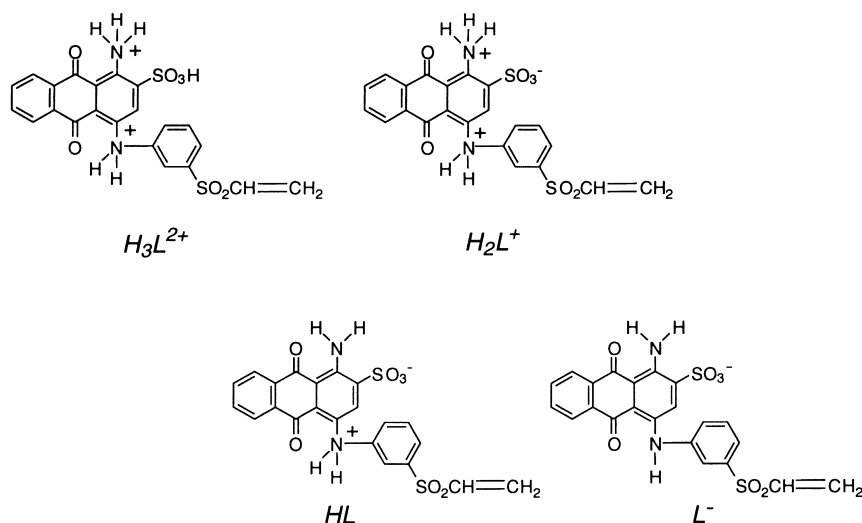
$\text{p}K_{a2} \sim 3.97$ . HL in Fig. 2 is present as a zwitterion and forms the species  $\text{L}^-$  with  $\text{p}K_{a3} = 6.37$  from the amino group. The species HL has a relevant concentration at pH values between 2 and 6.

The positively charged species  $\text{H}_3\text{L}^{2+}$  is shifted to more acid pH values than  $\text{H}_2\text{L}^+$  and these species coexist in solution with the neutral HL species.

The distribution of the surface species of hematite as a function of pH has already been reported (Bandara *et al.*, 1999). Neutral surface sites, denoted by  $>\text{FeOH}$ , predominate in the pH region between 6.5 and 11. The  $>\text{FeOH}_2^+$  sites increase from a negligible fraction at pH 8 to 50% at pH 6 and to 100% at pH 4. The  $>\text{FeO}^-$  fraction begins to be meaningful at pH > 8 reaching 100% at pH 14. The generalized two-layer model (diffuse/GTL) is used to model the hematite surface species (Stumm and Morgan, 1996). To calculate the surface species distribution of hematite the values considered were  $\text{p}K_a$  6.7 and 10.4, BET area of  $150 \text{ m}^2 \text{ g}^{-1}$  and  $4.7 \times 10^{-3} \text{ mol g}^{-1}$  of sites gram of  $\alpha\text{-Fe}_2\text{O}_3$ .

#### Modeling the interaction of Uniblue A and hematite

Figure 3(a) presents the modeling of the speciation of Uniblue A when interacting with hematite as a function of pH. The surface complexation taking place between Uniblue A and the hematite surface sites is analyzed in terms of equations (3)–(11). The criteria used to establish these equations are: (a) sorption is only possible at specific surface coordination sites; (b) sorption reactions can be described by mass law equations; (c) the surface complex modeling does not consider the charges of the dye species in solution and (d) the effect of surface charge on sorption is taken into account by applying a correction factor from the electric double-layer theory to the mass law constants for surface reactions (Diffuse/GTL) and finally (e) an incoming ligand like Uniblue A will coordinate to one or two Fe sites



Scheme 2.

forming a one or two Fe-centered surface complex. Fig. 3(a) involves the species  $>\text{FeOH}_2^+$ ,  $>\text{FeOH}$ ,  $>\text{FeL}$  complex,  $\text{L}^-$  and  $\text{HL}$ . The residual species are present at a very low concentration ( $<0.05 \text{ mM}$ ) and the experimental points overlap on a straight line at the lower end in Fig. 3(a).

The matrix used for the ChemEQL calculations takes into account only the hematite charges  $>\text{FeO}(-1)$ ,  $>\text{FeOH}(0)$ ,  $>\text{FeOH}_2^+(+1)$  and of the complexes  $>\text{FeHL}^+(+1)$ ,  $>\text{Fe}_2\text{HL}^{2+}(2)$ ,  $>\text{FeL}(0)$  and  $>\text{Fe}_2\text{L}^+(1)$ . The matrix is established with the known  $\text{pK}_a$  values for Uniblu A and hematite, as stated above. The  $K_{\text{eq}}$  values for the complexes  $>\text{FeHL}^+$ ,  $\text{Fe}_2\text{HL}^{2+}$ ,  $>\text{FeL}$  and  $>\text{Fe}_2\text{L}^+$  were found from the mass equations and the sites balance taking into account: (a) the amount of L (Uniblu A in solution) from spectral observations and (b) the surface active sites before and after Uniblu A adsorption on the oxide surface. Solving the four simultaneous equations (8)–(11) by MatLab 5.2 allowed to obtain the values: 8.66, 17, 5, 2.6 and 7.05 for  $K_{\text{eq}}$  of the complexes  $>\text{FeHL}^+$ ,  $>\text{Fe}_2\text{HL}^{2+}$ ,  $>\text{FeL}$  and  $>\text{Fe}_2\text{L}^+$ .

The reaction schemes 3–11 modeled in Fig. 3(a) follows the criteria outlined above.

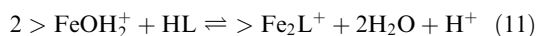
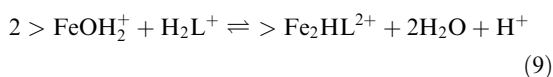
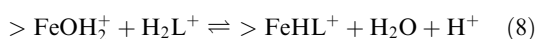
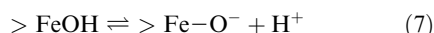
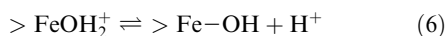
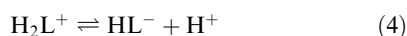
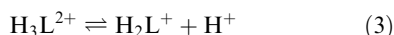


Fig. 3(b) can be understood in terms of reactions (3)–(11). This latter set of equations was found to match the experimental points obtained for the Uniblu absorption as a function of pH (Fig. 3(b)). The combination of reactions shown by equations (3) and (11) fits the experimental data and seem to be the reactions responsible for the observed absorption. Fig. 3b shows that Uniblu A adsorption begins at pH 8 and increases to pH 5.5 where it levels off. At pH  $>8$  no adsorption is observed since the adsorbent and adsorbate exist in their negative form:  $\text{L}^-$  and  $>\text{FeO}^-$ . The  $>\text{FeOH}_2^+$  interacts electrostatically with the Uniblu A negative  $\text{SO}_3^{2-}$ -group ( $\text{L}^-$ , Fig. 2) at pH  $<8$  leading to the adsorption of the Uniblu A on hematite. The adsorption of Uniblu A on

hematite proceeds with four possible complex stoichiometries (a) two complexes with a 1:1 ratio of Fe:Uniblu A ligand and (b) two further complexes with a 2:1 ratio of Fe and Uniblu. Surface complexes are denoted as  $>\text{FeHL}^+$ ,  $>\text{Fe}_2\text{HL}^{2+}$ ,  $>\text{FeL}$  and  $>\text{Fe}_2\text{L}^+$ .

#### Catalytic combustion of Uniblu A on hematite

The amount of  $\text{CO}_2$  for each sample (Fig. 4) was normalized to the weight of each of the tablets. Below  $200^\circ\text{C}$  ( $473 \text{ K}$ ), the quantity of gas collected was extremely small. At temperatures between 275 and  $400^\circ\text{C}$  in Fig. 3 about 40% of the initial C-content of the Uniblu A adsorbed on hematite was detected as  $\text{CO}_2$ . In addition, about 6% of the initial C-content (ashes) was found by elementary analysis on the hematite surface. But about 50% of the total organic carbon was transformed into smaller molecules which desorb from the hematite surface. These incomplete combustion gaseous by-products are reported in the section below. The units in the inset of Fig. 4 are  $\text{s}^{-1}$  because the reaction was observed to be pseudo-first order in excess  $\text{O}_2$  atmosphere.

Uniblu A was combusted in the absence of hematite to assess the influence of hematite on the combustion of Uniblu A. The control points (Ctrl) in Fig. 4 show the combustion in the absence of hematite. In this case the amounts detected were 2%  $\text{CO}_2$  at  $275^\circ\text{C}$  ( $548 \text{ K}$ ) and 27%  $\text{CO}_2$  at  $350^\circ\text{C}$  ( $623 \text{ K}$ ). The amounts of  $\text{CO}_2$  are far below the amounts of  $\text{CO}_2$  shown in Fig. 4 for the combustion of Uniblu A at the same temperatures. The C-ashes in this case were about 8% and the by-products of the order of 65% ( $350^\circ\text{C}$ ). The latter result shows the drastic enhancement of the amount of Uniblu A undergoing complete oxidation due to hematite during catalytic combustion. A much higher complete oxidation percentage is observed in terms of  $\text{CO}_2$  as compared to the case when the combustion was carried out in the absence of hematite.

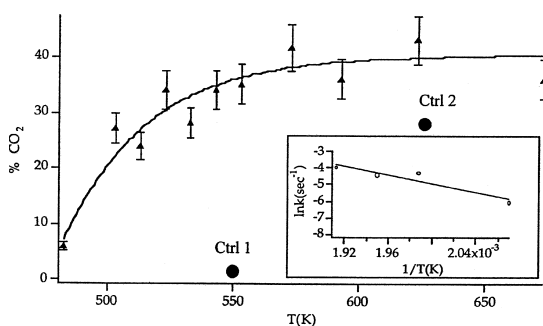


Fig. 4. Generation of  $\text{CO}_2$  in air during the catalytic combustion of Uniblu A adsorbed on hematite as a function of temperature. The control points (Ctrl) show the combustion in the absence of hematite. The inset shows the plot used for the determination of the activation energy ( $E_a$ ).

*System for thermal degradation studies coupled gas-chromatography and mass-spectrometry (STDS-GC-MS) measurements*

Figures 5 and 6 show the STDS-GC-MS chromatograms of the thermal products obtained for the Uniblu A alone and Uniblu A adsorbed on hematite as a function of three different temperatures. Tables 1 and 2 report the gaseous by-products found and report the structure of these compounds at 200, 300, 375, 450 and 600°C. By-product 10 in Table 2 is not observed

in Table 1. This by-product in the presence of hematite is formed at temperatures as low as 200°C (Table 2). In the absence of hematite it appears only at 600°C (Table 1). This latter effect is indicative of the favorable catalytic effect of the iron oxide during the combustion of Uniblu. In addition Table 2 shows the formation of chlorobenzene (by-product 10). This by-product is not found in the absence of hematite and can be ascribed to residual chloride content of iron oxide (Cornell and Schwertmann, 1980). During combustion processes chlorides in the presence

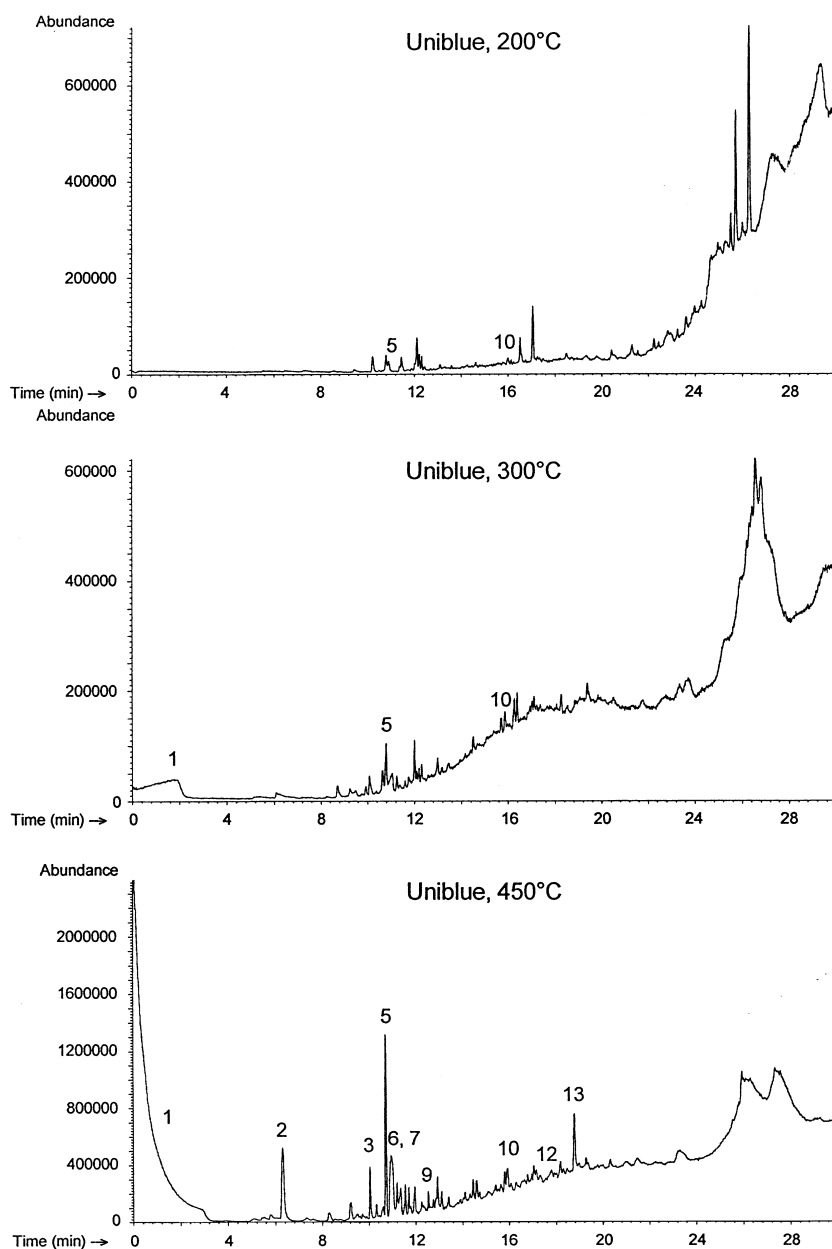


Fig. 5. STDS-GC-MS chromatograms of Uniblu A at 200, 300 and 450°C. For further details identifying the peaks see Table 1.



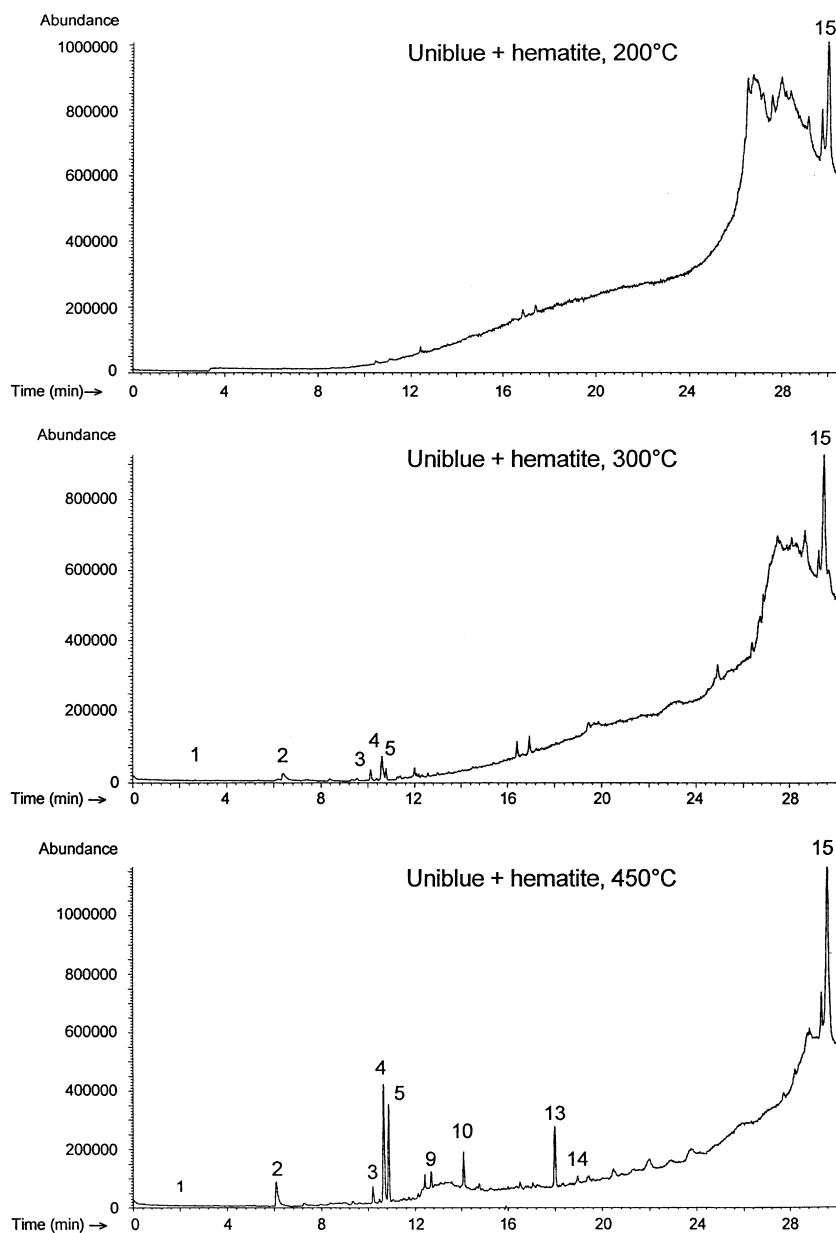


Fig. 6. STDS-GC-MS chromatograms of Unibblue A adsorbed on hematite at 200, 300 and 450°C. For further details identifying the peaks see Table 2.

Table 3. Surface properties of hematite determined by physisorption measurements before and after catalytic combustion cycles with Unibblue A at 273°C

	Hematite alone	Hematite + Unibblue	Cycle 1	Cycle 2
BET surface area ( $\text{m}^2 \text{g}^{-1}$ )	157.7	131.9	101.9	85.1
Micropore volume ( $\text{cm}^3 \text{g}^{-1}$ )	0.0046	0.0043	0.0024	0.0020
Micropore area ( $\text{m}^2 \text{g}^{-1}$ )	13.37	8.17	1.58	1.20
Average pore diameter ( $\text{\AA}$ )	171.0	171.5	165.2	170.1
Porosity (%)	70.8	70.5	65.4	62.8

of iron give rise to the formation of HCl which is transformed into molecular chlorine leading to the formation of chlorinated organic compounds. In addition, the formation of additional organic

compounds like formaldehyde, acetaldehyde and glyoxal and glyoxal-derivatives has been detected besides the compounds reported in Tables 1 and 2.

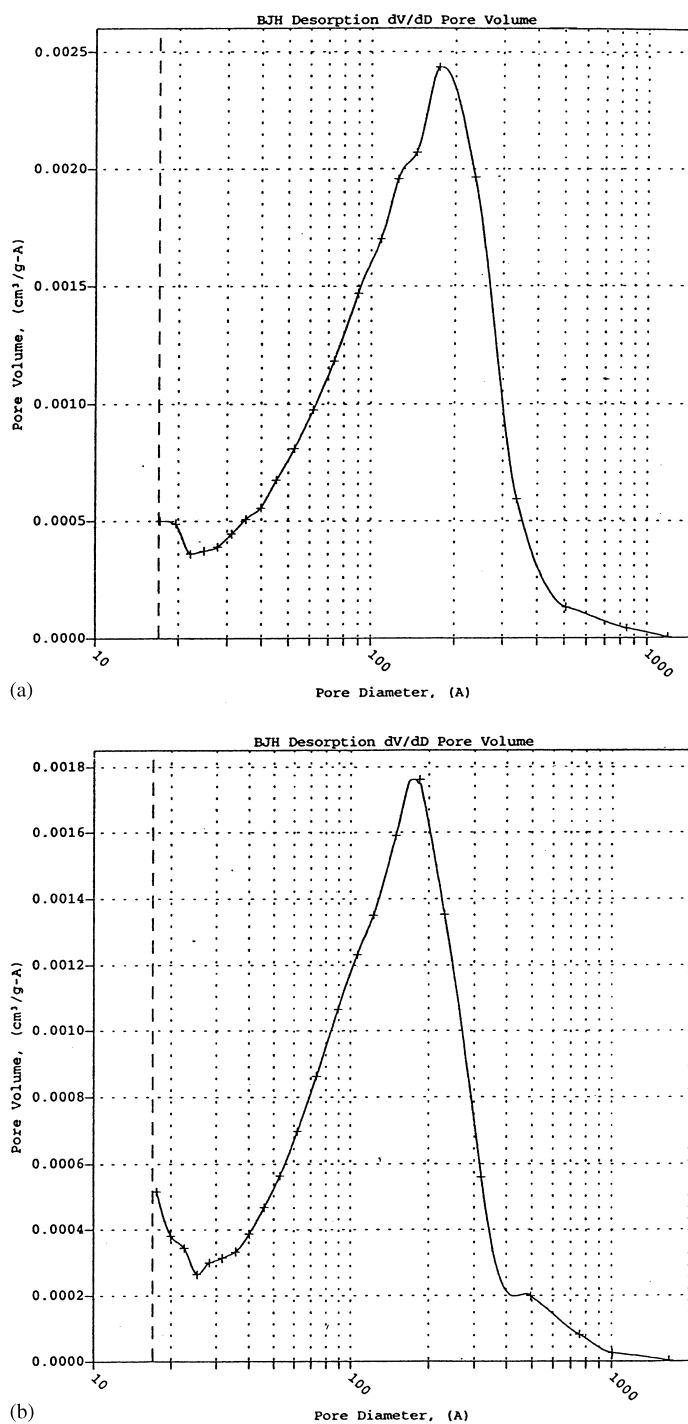


Fig. 7. (a) Pore volume as a function of pore diameter of hematite loaded with Uniblue A after the first catalytic combustion at 275°C. (b) Pore volume as a function of pore diameter of hematite loaded with Uniblue A after the second catalytic combustion at 275°C.

The compounds evolved in the catalytic combustion as shown in Table 2 are irritating if inhaled in large amounts leading to respiratory disorders. The former consideration applies to: benzene, thiophene, phenol, aniline, naphthalene, chlorobenzene, acetalde-

hyde, acetone, acetonitrile and acetic acid of Tables 1 and 2 (Merck Index, 1989). Open-air catalytic combustion of Uniblue A will not be hindered by the former consideration. This is due to the relative amounts involved in open-air combustions.

*Physical characterization of the catalyst by N<sub>2</sub> physisorption*

The specific surface area, the pore average size diameter and the porosity of hematite with adsorbed Uniblue A before and after two catalytic combustion cycles of Uniblue A at 273°C do not show any meaningful variation. This is shown in Table 3. For hematite alone the values found are shown in the first column. The pore average size diameter is seen to vary between 171.0 and 170.5 Å for hematite and hematite with Uniblue A, respectively. No change occurs in the pore size after the first and second catalytic cycles as can be seen from Figs 7a and b, the system being hematite with Uniblue A. The parameters in Table 3 were calculated as reported recently by our group (Bacsa and Kiwi, 1998). The hematite density of 5.82 g cm<sup>-3</sup> was used to calculate the sample porosity.

### CONCLUSION

Adsorption and catalytic combustion of the reactive dye Uniblue A has been studied on hematite. Complete combustion of Uniblue A (as reflected by the amount of CO<sub>2</sub> evolved) was observed to be the preferential process for Uniblue A adsorbed on hematite. Incomplete oxidation products, on the other hand, predominate when Uniblue A was combusted in the absence of hematite. At the same temperatures the formation of gaseous by-products in the latter case was observed to be higher than in the presence of hematite. Modeling of the surface speciation and the Uniblue A charged-ions in solution allows for a quantitative prediction of the amount of dye adsorbed as a function of pH. In the main, electrostatic effects between the oxide surface and the Uniblue A species on the hematite surface determine the extent of adsorption as a function of pH. The activation energy was determined for the catalytic combustion of the adsorbed Uniblue A on hematite. Physical characterization of the catalyst by N<sub>2</sub> physisorption was carried out and gives insight into the nature of the surface responsible for the catalytic combustion.

*Acknowledgements*—The financial support of the European Communities Environmental Program ENV-CT-95-0064

(OFES Contract No. 96.350 Bern) is gratefully acknowledged.

### REFERENCES

- Bacsa R. and Kiwi J. (1998) Effect of the rutile phase on the photocatalytic properties of nanocrystalline titania during the degradation of p-coumaric acid. *Appl. Catal. B.* **16**, 19–29.
- Barret E., Joyner L. and Halenda P. (1951) The calculation of pore size distribution from adsorption data. *J. Amer. Chem. Soc.* **73**, 373–381.
- Bandara J., Mielczarski A. J. and Kiwi J. (1999) Molecular mechanism of surface recognition. Azo-dyes degradation on Fe, Ti, and Al-oxides through metal sulfonate complexes. *Langmuir* **15**, 7670–7679.
- Camp S. and Sturrock P. (1990) Covalent reactive dye-fiber linkage for vinyl sulfone remazols. *Water Res.* **24**, 1275–1281.
- Cornell R. and Schwertmann U. (1980) Preparation of large surface area iron-oxides. *Colloid Polym. Sci.* **258**, 1171–1225.
- Ganesh R., Boardman G. and Nicholson D. (1994) Fate of azo-dyes in sludges. *Water Res.* **28**, 1367–1376.
- Herrera F., Kiwi J., Lopez A. and Nadtochenko V. (1999) Photochemical decoloration of remazol brilliant blue and uniblue A in the presence of Fe<sup>3+</sup> and H<sub>2</sub>O<sub>2</sub>. *Environ. Sci. Technol.* **33**, 3145–3152.
- Hoechst Portuguesa, S. A., 1997. Aqua Ambiente, Apartado 6, P-2726. Martins Cedex, Portugal.
- Ince N., Stefan M. and Bolton J. (1997) UV/H<sub>2</sub>O<sub>2</sub> Degradation and toxicity reduction of textile azo dyes: remazol black-B, a case study. *J. Adv. Oxid. Technol.* **2**, 442–448.
- Loneragan T., Panow A., Jones C. and Mainwaring D. (1995) Physiological and degradative behavior of white-rot fungus in a 200 liter packed bed bioreactor. *Fermentation Technol.* **5**, 107–117.
- Mascolo G., Spinosa L., Lolito V., Mininni G. and Bagnolo G. (1997) Lab-scale evaluations on formation of products of incomplete combustion in hazardous waste incineration: influence of process variables. *Water Sci. Technol.* **36**, 219–227.
- Merck Index*, 1989. Merck and Co. Rahway, NJ, USA.
- Pasti M. and Crawford D. (1991) Relationships between the abilities of streptomycetes to decolorize anthron-type dye and degrade lignocellulose. *Can. J. Microbiol.* **37**, 902–907.
- Pulgarin C. and Kiwi J. (1996) Overview on photocatalytic and electrocatalytic treatment of industrial non-biodegradable pollutants and pesticides. *Chimia* **50**, 50–55.
- Roques H. (1996) *Chemical Water Treatment Principles and Applications*. VCH, Weinheim, Germany.
- Stumm W. and Morgan J. (1996) *Aquatic Chemistry*. Wiley Interscience, New York.
- Zollinger H. (1987) *Properties and Applications of Organic Dyes and Pigments*. VCH, Pub, New York.